Mobility spatial distribution function: Comparative method for conjugated polymers/molecules

Noam Rappaport, Yehoram Bar, Olga Solomeshch, and Nir Tessler[a)]
Microelecronics and Nanoelectronics Centers, Electrical Engineering Department, Technion Israel Institute of Technology, Haifa 32000, Israel

The authors report improved method for extracting mobility spatial distribution function that accounts for the finite light-absorption depth. They employ step function light excitation and use the photocurrent temporal response to extract the electrons' mobility spatial distribution function (MDF). This directly measures the relevant electronic disorder in amorphous conjugated polymers. Comparing two different polymers shows that qualitative analysis of field effect transistor data is in good agreement with the quantitative analysis provided by the MDF concept/method. The better uniformity of the electronic properties found in green polypnenylene vinylene is a clear indication for its better performance and lifetime. © 2006 American Institute of Physics.
[DOI: 10.1063/1.2422904]

The importance of organic photocells[1–5] is gradually rising as indicated by the steady increase in reports concerning material synthesis[6–8] or material composite design[9–11] which are specifically targeting photocell functionalities. It was recently shown that the performance of low mobility material based photocells is governed entirely by the slowest charge mobility and the target mobility value for AM1.5 excitation power of $\mu_{\min} = 10^{-2}$ cm^2/V s has been derived based on charge recombination analysis.[8] It has also been shown that in materials where Langevin recombination takes place, it becomes significant at about the same power level as space charge effects,[12] thus allowing the use of expressions derived based on Langevin recombination to predict the onset of space charge effects. In other words, understanding and characterizing the mobility in solar cell devices are critical for the development of better devices and materials.

We have recently presented a method for analyzing the transport of the slower (limiting) charge carrier in thin films and introduced the mobility spatial distribution function (MDF) concept.[13] Since this method uses a step function light excitation (i.e., it is turned on instantaneously and kept at the on state until all transients end), it is 100% compatible with normal device operation and one can set the input power (step height) to match relevant operation conditions. The MDF concept is based on the notion that a disordered semiconductor can be considered homogeneous only on very large scales and that on the nanometer scale spatial inhomogeneity of the electronic properties takes place. If one considers a relatively small volume then its properties would depend on where on the sample this volume is being picked from thus leading to different mobility pathways or to a spatial distribution of mobility values.[13]

It was shown that using this concept, one can write a straightforward expression for the time dependence of the photocurrent that follows a step function excitation [see Eq. (1)]. The assumption in previovs paper[13] was that the slow charge carriers are generated very close to the opposite contact [as in electrons close to the indium tin oxide (ITO) an-

ode, top of Fig. 1(b)], and thus the expression for the current could be mathematically manipulated to produce an analytic formula to extract the mobility distribution function of a given device. Here we lift this assumption and present an expression that accounts for the finite absorption length [bottom of Fig. 1(b)], and due to the relatively thick device we do not include interference effects. This inclusion of the finite absorption length not only improves the quality of the extracted MDF but also allows us to compare two different polyphenylene vinylene (PPV) polymers and demonstrate that the MDF method is practically useful.

Assuming all charges are generated near the ITO contact and that the electrons are the slow carriers, we have derived[13]

$$J_e(t) = APq \left\{ \int_{d^2/Vt}^{\infty} g(\mu_e) d\mu_e + \int_0^{d^2/Vt} g(\mu_e) \frac{t}{t_{\mathrm{tr}}(\mu_e)} d\mu_e \right\},$$

(1)

whereas J_e is the electron current density, $g(\mu_e)$ is the distribution function for the electron mobility pathways, $t_{\mathrm{tr}}(\mu_e)$ is the transit time across the device for an electron with mobility μ_e ($t_{\mathrm{tr}}(\mu_e) = (d^2/\mu_e V)$), d is the device thickness, q is the electron charge, P is the incident light intensity, and A is the carrier pair generation efficiency (number of electron-hole pairs generated per unit of incident intensity).

To account for the finite absorption length the above expression needs to be modified. We first write the expression for the current due to electrons that are generated at a distance "s" from the cathode and are swept towards it.

$$J_e(t,s)ds = I_0 q e^{-\alpha(d-s)} \frac{s}{d} \left\{ \int_{sd/Vt}^{\infty} g(\mu_e) d\mu_e \right.$$
$$\left. + \int_0^{sd/Vt} g(\mu_e) \frac{t}{t_{\mathrm{tr}}(\mu_e, s)} d\mu_e \right\} ds.$$

(2)

Where now $t_{\mathrm{tr}}(\mu_e, s) = (ds)/(\mu_e V)$ and $I_0 e^{-\alpha(d-s)} ds$ is the carrier generation rate at the ds slice. As in Ref. 13, we do not account for diffusion which is justified as long as the

a)Electronic mail: nir@ee.technion.ac.il; URL: www.ee.technion.ac.il/orgelect
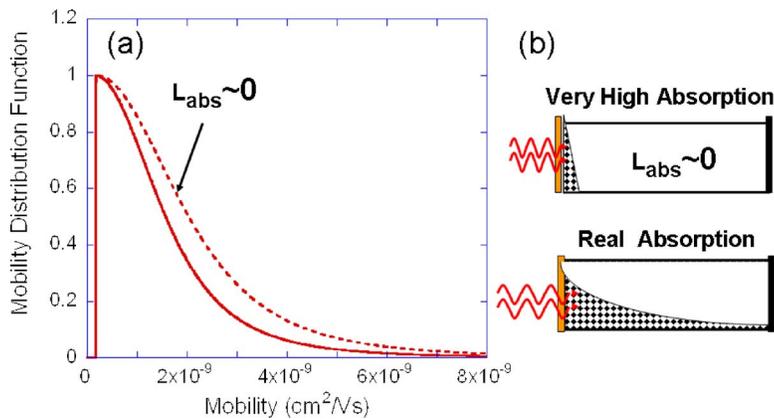
FIG. 1. (Color online) (a) Electron mobility distribution function extracted for MEH-PPV based device. The dashed line is derived using Eq. (1) and does not account for the finite absorption depth of the polymer. The full line is derived using Eq. (3) and represents the true MDF. (b) Illustration of a device with infinitely high absorption coefficient (top) and a more realistic case (bottom).

total electric field (built in+applied) is larger than $\sim 10^4$ V/cm. The transient current can therefore be found by integrating along the device,

$$J_e(t) = I_0 q \int_0^d e^{-\alpha(d-s)} \frac{s}{d} \left\{ \int_{sd/Vt}^{\infty} g(\mu_e) d\mu_e \right.$$
$$\left. + \frac{tV}{sd} \int_0^{sd/Vt} g(\mu_e) \mu_e d\mu_e \right\} ds. \tag{3}$$

Equation (3) is an explicit expression describing the photocurrent response to a step function light excitation in the presence of spatial inhomogeneity $g(\mu)$ and accounting for the potentially significant absorption length $L_{abs} = \alpha^{-1}$. Unfortunately, once we introduce the absorption depth effect we are not able anymore to manipulate the equation to provide an analytic expression for the extraction of the MDF from the photocurrent temporal response. However, based on the analysis presented in Ref. 13, we found that the MDF tends to have a general functional form that enables us to relatively quickly extract $g(\mu)$ by numerically fitting Eq. (3) to the measured current response. This functional form of the MDF is

$$g(\mu_e) = \begin{cases} g_0 \left[\dfrac{(\mu_e - \mu_{e0})^2}{\sigma_1^2} + 1 \right]^{-2} & \text{for } \mu_e \geq \mu_{e0} \\[2ex] g_0 \left[\dfrac{(\mu_e - \mu_{e0})^2}{\sigma_2^2} + 1 \right]^{-2} & \text{for } 0 \leq \mu_e \leq \mu_{e0.} \end{cases}$$
$$\tag{4}$$

We arrived at this expression through the observation that the first derivative of the measured current highly resembles a Lorenzian function. Assuming that the first derivative is indeed a Lorenzian function, then applying Eq. (2) in Ref. 13 results in a formula of the type shown here in Eq. (4). While we can not physically justify this expression, it reproduces very well the MDF reported in Ref. 13 and it also allows us to excellently fit Eq. (3) here to the measured data.

In Fig. 1 we plot the MDF that was extracted from the temporal current response data of a MEH-PPV based device under short circuit conditions (details of the measurement technique and device preparation can be found in Ref. 13). The dashed line is the MDF that was extracted using Eq. (1) and the full line is when Eq. (3), that accounts for L_{abs}, was employed. As the figure shows, if the fact that part of the carriers are being generated in the bulk of the sample is not being accounted for (as in the dashed line), then these carriers would appear as "fast paths" producing an extended tail

towards the high mobility range. The difference between the dashed and full lines demonstrates the importance of accounting for the absorption depth if one is seeking quantitative data for comparative analysis. The σ parameter associated with the MDF derived accounting for absorption is $\sigma_1 = 2.2 \times 10^{-9}$ cm^2/V s, while for the MDF derived without accounting for it $\sigma_{1_{L_{abs}=0}} = 3 \times 10^{-9}$ cm^2/V s.

In order to verify that the MDF concept and method can provide useful information regarding the sample and material properties (quality) we compare two materials: green PPV and MEH-PPV. We first present data extracted using an entirely different device structure and method. Next, we show that there is qualitative good agreement. Figures 2(a) and 2(b) show the chemical structure of green PPV and MEH-PPV, respectively (more details regarding the green-PPV material family can be found in Ref. 14. Figure 2(c) shows the field effect hole mobility of the two polymers extracted from the transfer characteristics measured in a bottom contact configuration (exact FET structure and measurement procedure are described in Ref. 15). The figure shows the known phenomena of gate (charge density) dependent mobility found in disordered amorphous materials. It is established by now[16–19] that there is a direct relation between the degree of density dependence and the amount of disorder found in the material. Figure 2(c) thus serves as an indication, independent of the MDF method, that MEH-PPV is more electronically disordered compared to green PPV.

m=3% n=48.5% o=48.5%
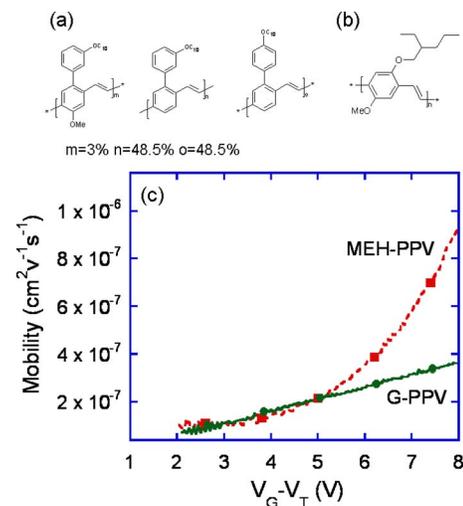
FIG. 2. (Color online) (a) Chemical structure of green PPV. (b) Chemical structure of MEH-PPV. (c) Hole field effect mobility extracted from the transfer characteristics of bottom contact FETs (Ref. 15).
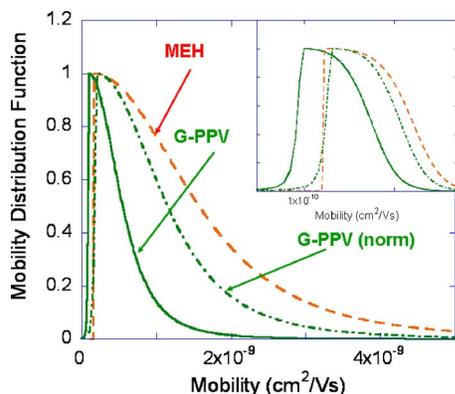
FIG. 3. (Color online) Electron mobility distribution function derived for green PPV (full line) and MEH-PPV (dashed line). The dash-dot line is the green-PPV's function with its x axis normalized (stretched) to overlap the low mobility side of the MEH-PPV's function. The inset shows the same curves on a semilog X scale. The device structure was glass ITO polyethylenedioxythiophene polymer aluminum. The thickness of the green-PPV layer was ~150 nm and of the MEH-PPV layer was ~300 nm.

After establishing that field effect measurements indicate that MEH-PPV is more electronically disordered compared to green PPV we move to quantifying this difference by examining the electron mobility distribution function in a solar cell device configuration. Figure 3 shows the mobility distribution function derived for green PPV (full line) and MEH-PPV (dashed line). The dash-dot line is the green-PPV's function with its x axis normalized (stretched) to overlap the low mobility side of the MEH-PPV's function.

Comparing the normalized green-PPV MDF and the MEH-PPV MDF it is evident that the distribution function of the green PPV is significantly narrower. In fact, the σ_1 parameter that characterizes the high mobility side tail takes the values of 2.2×10^{-9} and 1.6×10^{-9} cm^2/V s for the MEH-PPV and the normalized green-PPV functions, respectively.

To conclude, we have introduced an improved method for extracting the mobility spatial distribution function which accounts for the finite absorption depth in thin film devices. We have shown that if the absorption depth, which can be on the same order of the device thickness, is not accounted for, then the fast mobility tail is exaggerated. Two PPV materials were tested and good agreement with FET data was found. By comparing the two materials we quantified the difference and found that in green PPV the electronic disorder (σ_1) is about 30% less than that found in MEH-PPV. The MDF method is a fast and direct method for characterizing the electronic uniformity (electronic order) of materials thus being a useful tool for material development and screening. Finally, we suggest that even robust models (as the one for deriving the Einstein relation[20]) need rechecking in the context of thin films.

[1] C. W. Tang, Appl. Phys. Lett. **48**, 183 (1986).
[2] C. J. Brabec and S. N. Sariciftci, Monatsch. Chem. **132**, 421 (2001).
[3] W. U. Huynh, J. J. Dittmer, and A. P. Alivisatos, Science **295**, 2425 (2002).
[4] A. Moliton and J. M. Nunzi, Polym. Int. **55**, 583 (2006).
[5] G. Li, V. Shrotriya, J. S. Huang, Y. Yao, T. Moriarty, K. Emery, and Y. Yang, Nat. Mater. **4**, 864 (2005).
[6] G. Yu, J. Wang, J. McElvain, and A. J. Heeger, Adv. Mater. (Weinheim, Ger.) **10**, 1431 (1998).
[7] M. Gratzel and K. Kalyanasundaram, Curr. Sci. **66**, 706 (1994).
[8] N. Rappaport, O. Solomesch, and N. Tessler, J. Appl. Phys. **98**, 033714 (2005).
[9] A. C. Arias, J. D. Mackenzie, R. Stevenson, J. J. M. Halls, M. Inbasekaran, E. P. Woo, D. Richards, and R. H. Friend, Macromolecules **34**, 6005 (2001).
[10] J. J. M. Halls, C. A. Walsh, N. C. Greenham, E. A. Marseglia, R. H. Friend, S. C. Moratti, and A. B. Holmes, Nature (London) **376**, 498 (1995).
[11] G. Yu, J. Gao, J. C. Hummelen, F. Wudl, and A. J. Heeger, Science **270**, 1789 (1995).
[12] N. Tessler and N. Rappaport, Appl. Phys. Lett. **89**, 013504 (2006).
[13] N. Rappaport, O. Solomesch, and N. Tessler, J. Appl. Phys. **99**, 064507 (2006).
[14] H. Becker, H. Spreitzer, W. Kreuder, E. Kluge, H. Schenk, I. Parker, and Y. Cao, Adv. Mater. (Weinheim, Ger.) **12**, 42 (2000).
[15] S. Shaked, S. Tal, Y. Roichman, A. Razin, S. Xiao, Y. Eichen, and N. Tessler, Adv. Mater. (Weinheim, Ger.) **15**, 913 (2003).
[16] Mcjm Vissenberg and M. Matters, Phys. Rev. B **57**, 12964 (1998).
[17] Y. Roichman, Y. Preezant, and N. Tessler, Phys. Status Solidi A **201**, 1246 (2004).
[18] Nir Tessler and Yohai Roichman, Compr. Rev. Food Sci. Food Saf. **6**, 200 (2005).
[19] C. Tanase, E. J. Meijer, P. W. M. Blom, and D. M. de Leeuw, Phys. Rev. Lett. **91**, 216601 (2003).
[20] Y. Roichman and N. Tessler, Appl. Phys. Lett. **80**, 1948 (2002).